Proceedings of the International Conference on Oxide Materials for Electronic Engineering (OMEE 2021)

Synthesis and Electrochemical Properties of $Li_yCa_xNd_{1-x}MnO_3$ Solid Solution

V.M. Kordan[a,*], O.I. Zaremba[a], P.Yu. Demchenko[a] and V.V. Pavlyuk[a,b]

[a] *Faculty of Chemistry, Ivan Franko National University of Lviv, Kyryla i Mefodiya St., 6, 79005 Lviv, Ukraine*
[b] *Institute of Chemistry, Jan Długosz University of Częstochowa, Armii Krajowej Ave, 13/15, 42200 Częstochowa, Poland*

Doi: 10.12693/APhysPolA.141.273 *e-mail: vasyl.kordan@lnu.edu.ua

New $Li_yCa_xNd_{1-x}MnO_3$ solid solutions were synthesized by electrochemical insertion of Li in the structure of the Ca–Nd–Mn–O system ceramics. The starting 1:1:3-oxides were synthesized in a solid-state reaction. The composition of the $Ca_{0.5}Nd_{0.5}MnO_3$, $Ca_{0.3}Nd_{0.7}MnO_3$ and $Ca_{0.05}Nd_{0.95}MnO_3$ samples was confirmed by X-ray fluorescent spectroscopy and energy-dispersive X-ray spectroscopy. The obtained ceramics are characterized by orthorhombic symmetry ($GdFeO_3$-type structure, space group *Pnma*, Pearson's code *oP*20, $Z = 4$). Insertion of Li into the voids of oxide phase takes place during the discharge process at a potential below 3.5 V (Li-metal as an anode material and studied ceramics as cathode material). The compositions of Li-containing solid solutions are $Li_{0.057}Ca_{0.5}Nd_{0.5}MnO_3$, $Li_{0.091}Ca_{0.3}Nd_{0.7}MnO_3$ and $Li_{0.113}Ca_{0.05}Nd_{0.95}MnO_3$. The X-ray phase and structural analysis showed the formation of phases with an increased unit cell and the appearance of an amorphous halo which is a by-products of the reaction between the electrode surface and electrolyte. The scanning electron microscopy method showed the formation of Li-containing aggregates with dimensions of 1–3 μm. The small grains have a block-like shape and a diameter of < 400 nm.

topics: perovskites, solid solution, lithiation

1. Introduction

Complex oxides with a 1:1:3 composition belong to the perovskite family, the investigation of which takes into account the variety of their applications. Due to the mixed cation oxidation state, such perovskites have interesting physical properties. The most frequently studied are magnetic, photoelectric (energy accumulation), catalytic, as electrodes in solid oxide fuel cell (energy transformation) [1–5]. The characteristics and parameters of perovskites as electrodes for lithium-ion batteries are described in [6, 7].

Most of the metal hydride, Li-ion, Na-ion, Mg-ion batteries use intermetallic phases or composites as anodes (negative electrode). Intermetallic compounds with large octahedral or tetrahedral voids are suitable for the H, Li, Na or Mg insertion [8–11]. As a result, the solid solutions of inclusion or substitution are formed. Most cathode materials for Li-ion and Na-ion batteries are based on layered or distorted oxides. During the discharge, the process of Li-intercalation in the structure of ceramics take place. In this paper, the structural investigations and electrochemical properties of the $Li_yCa_xNd_{1-x}MnO_3$ solid solution are discussed.

2. Experimental

The starting oxides were synthesized by solid-state reaction, starting from corresponding quantities of $CaCO_3$, Nd_2O_3 and Mn_2O_3 powders in two stages at 1000 and 1200°C. The duration of each stage was 24 and 8 h, respectively.

The phase and structural analysis of the samples before and after the electrochemical processes was carried out mainly by the powder X-ray diffraction using STOE STADI P diffractometer (Cu K_{α_1} radiation, λ=1.54060 Å, $5° \leq 2\theta \leq 100°$, monochromator Ge(111), T=292 K). The Li-containing ceramics before the X-ray diffraction measurement were mixed with dry indifferent oil to avoid oxidizing in air. The refinement of the crystal structure (Rietveld method) was performed using the FULLPROF program [12]. The qualitative and quantitative composition of the observed phases was studied using scanning electron microscope TESCAN Vega3 LMU (Oxford Instruments energy dispersive X-ray analyser, Aztec ONE system). The SE-detector characterizes the morphological contrast of the studied surface, the BSE-detector characterizes the contrast between the phases with different element content. X-ray fluorescent spectroscopy

(spectrometer ElvaX Pro) was used for the investigation of the integral composition of electrode materials before and after lithiation.

Electrochemical lithiation of the $Ca_xNd_{1-x}MnO_3$ solid solution was carried out in two-electrode Swagelok-type cells [13]. The battery prototype consisted of a negative electrode (metallic Li, > 99 wt.% of purity, commercial) and a positive electrode containing 0.3 g of studied oxides. A bulk polycrystalline sample was carefully ground, mixed with electrolyte, pressed into a cylinder with 1 mm of length and 1 cm of diameter and placed in to prototype. A separator (Celgard 2400, commercial) soaked in 1 M Li[PF_6] solution in aprotic solvents dimethyl carbonate and ethylene carbonate (commercial) was placed between the electrodes to avoid contact. Chronopotentiograms of the Li-ion battery prototypes were obtained in the galvanostatic regime using the 2-channel galvanostat MTech G410-2 [14]. The amount of Li per formula unit (notation [Li/f.u.]) was determined for the studied electrodes using Faraday's formula, where Li-content is directly proportional to the discharge time. The discharging time is from 11.4 for the $Ca_{0.5}Nd_{0.5}MnO_3$ electrode to 22.2 h for the $Ca_{0.05}Nd_{0.95}MnO_3$ electrode. The charging time is less (≈ 80% of discharging time).

The electrochemical reactions that occur on the cathode (positive electrode) and anode (negative electrode) can be presented by the following scheme

$$\text{Cathode}: \quad Ca_xNd_{1-x}MnO_3 + y\text{Li}^+ + y\bar{e} \underset{\text{charge (delithiation)}}{\overset{\text{discharge (lithiation)}}{\rightleftarrows}} \text{Li}_y^{\delta+}Ca_xNd_{1-x}MnO_3 \tag{1}$$

$$\text{Anode}: \quad \text{Li} \underset{\text{charge (delithiation)}}{\overset{\text{discharge (lithiation)}}{\rightleftarrows}} y\text{Li}^+ + y\bar{e} \tag{2}$$

3. Results and discussion

X-ray phase analysis of the synthesized samples showed that the starting ceramics contain only $Ca_xNd_{1-x}MnO_3$ solid solution. The samples revealed orthorhombic $GdFeO_3$ structure (Pearson symbol *oP*20, space group *Pnma*). An increase in the cell parameters was observed with an increase of the neodymium content in the sample (Table I). After lithiation, small amounts of unidentified phases were also observed with amorphous halo with low intensity peaks on a small angel area (5–25° 2θ). The new phases crystallized on the surface of grains probably are by-products of the interaction of the surface and components of the electrolyte. We assume that these interphases can be destroyed during intercalation/deintercalation of lithium. The parameters of the unit cell also increased after the inclusion of lithium in the structure of the solid solution $Ca_xNd_{1-x}MnO_3$ (for all investigated x values) (see Table I). The XRD powder patterns of the studied samples before and after lithiation are presented in Fig. 1.

The composition of the studied oxides was confirmed by spectral methods. The integral composition (cation ratio Ca/Nd/Mn) of $Ca_xNd_{1-x}MnO_3$ ceramics before lithiation from X-ray fluorescent spectroscopy is 0.56/0.500/0.97, 0.28/0.68/1.03, and 0.06/0.92/1.05 for x = 0.5, 0.3, and 0.05, respectively. Composition from energy-dispersive X-ray spectroscopy also correlates well with the nominal composition of the samples. After lithiation, the compositions of cathode materials practically do no differ from as-cast samples and are $Ca_{9.1}Nd_{8.9}Mn_{20.6}O_{61.4}$, $Ca_{7.1}Nd_{10.9}Mn_{19.4}O_{62.6}$ and $Ca_{1.1}Nd_{18.7}Mn_{20.1}O_{60.1}$ for x = 0.5, 0.3 and 0.05, respectively (composition without the C, F, O, P-elements from the electrolyte). So, the compositions of Li-containing solid solutions are $Li_{0.057}Ca_{0.5}Nd_{0.5}MnO_3$, $Li_{0.091}Ca_{0.3}Nd_{0.7}MnO_3$ and $Li_{0.113}Ca_{0.05}Nd_{0.95}MnO_3$ (1.1, 1.8 and 2.3 at.% Li). The specific capacity of the studied electrodes materials not exceeds 15–16 mAh/g.

The elemental mapping of lithiated samples is presented in Fig. 2. It should be noted that adsorption of electrolyte on the surface is the biggest for the $Ca_{0.5}Nd_{0.5}MnO_3$-based electrode. These by-products films passives the electrode grains. Probably it is a reason why the amount of the intercalated Li is low.

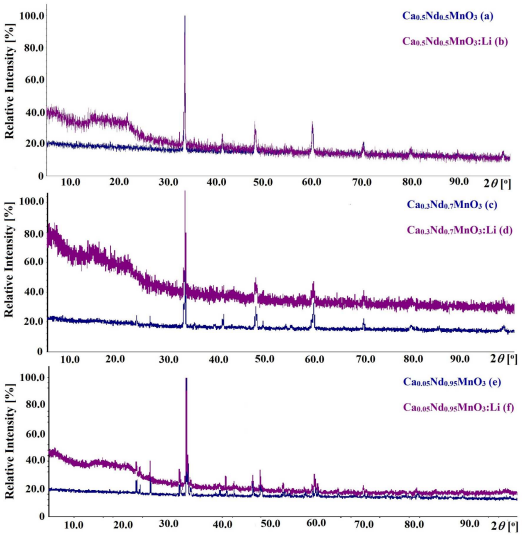

Fig. 1. XRD powder patterns of the $Ca_xNd_{1-x}MnO_3$ samples as-cast (a, c, e) and after lithiation (b, d, f).

TABLE I

Cell parameters of $Ca_xNd_{1-x}MnO_3$ ceramics before and after electrochemical lithiation.

Starting composition of $Ca_{1-x}Nd_xMnO_3$	Cell parameters		
	Before litiation	After lithiation	$\Delta V/V$ [%]
$x = 0.5$, $Ca_{0.5}Nd_{0.5}MnO_3$	$a = 5.3891(7)$ Å, $b = 7.5852(10)$ Å, $c = 5.3731(7)$ Å, $V = 219.64(5)$ Å^3	$a = 5.3953(12)$ Å, $b = 7.5908(17)$ Å, $c = 5.3766(11)$ Å, $V = 220.20(8)$ Å^3	0.25
$x = 0.3$, $Ca_{0.3}Nd_{0.7}MnO_3$	$a = 5.4569(5)$ Å, $b = 7.6484(7)$ Å, $c = 5.4068(4)$ Å, $V = 225.66(3)$ Å^3	$a = 5.4623(14)$ Å, $b = 7.652(2)$ Å, $c = 5.4102(12)$ Å, $V = 226.14(10)$ Å^3	0.21
$x = 0.05$, $Ca_{0.05}Nd_{0.95}MnO_3$	$a =5.6796(3)$ Å, $b =7.5858(4)$ Å, $c =5.4107(2)$ Å, $V =233.118(18)$ Å^3	$a = 5.6929(6)$ Å, $b = 7.6019(8)$ Å, $c = 5.4223(5)$ Å, $V = 234.66(4)$ Å^3	0.66

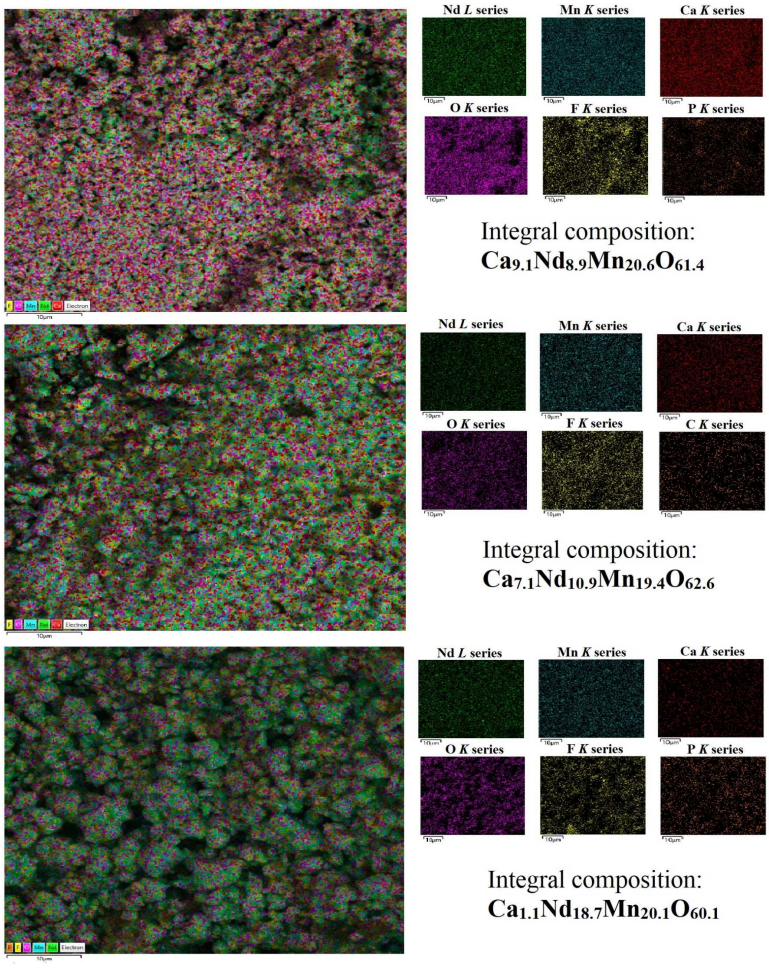

Fig. 2. Elemental mapping (EDX) for $Li_yCa_{1-x}Nd_xMnO_3$ samples (after 50 cycles of lithiation/delithiation).

In Fig. 3, SEM-images of the $Ca_{0.05}Nd_{0.95}MnO_3$ polycrystalline sample before and after lithiation are presented. We observed a change of surface morphology and grain sizes. Before lithiation, the block-like particle size is 3–6 μm and after lithiation, it is 1–3 μm. Small grains have diameter of < 400 nm and form big aggregates. We believe that increasing the duration of lithiation/delithiation experiment will cause more amorphization and the particle size will be less than 100 nm.

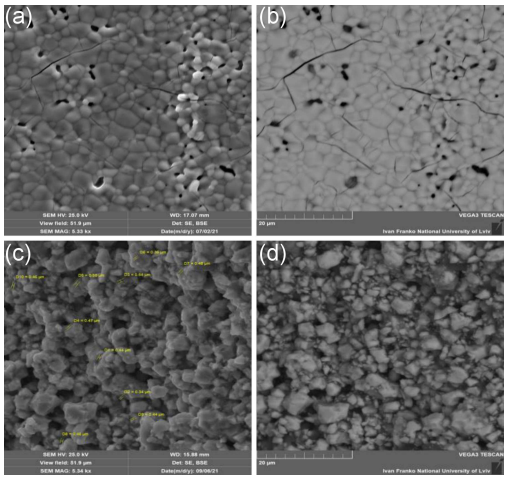

Fig. 3. SEM-images (SE- and BSE-detectors) of the $Ca_{0.05}Nd_{0.95}MnO_3$ (a, b) and $Li_xCa_{0.05}Nd_{0.95}MnO_3$ after 50 cycles of discharging/charging (c, d) samples.

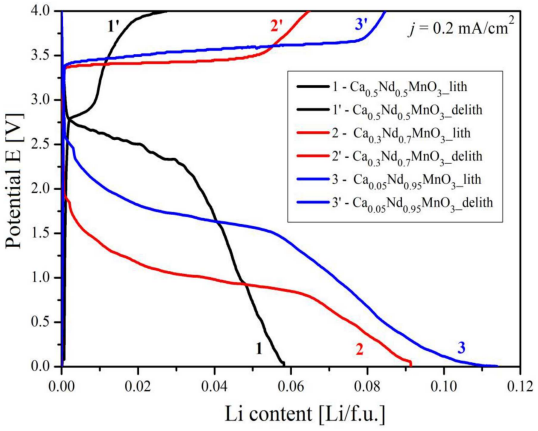

Fig. 4. Selected charge and discharge curves for battery prototype with cathode materials based on $Ca_{1-x}Nd_xMnO_3$solid solutions.

Insertion of Li into the voids of oxide phases takes place during discharge process at a potential below 3.5 V (Fig. 4) [15]. We consider that the crystal structure of cathode materials is not destroyed during electrochemical processes. The formed $Li_yCa_xNd_{1-x}MnO_3$ solid solution can be interpreted as a filled-up $GdFeO_3$ orthorhombic perovskite. Insertion of lithium into the structure presumably occurs in the voids between the layers of large cations (Ca/Nd) and the layers of octahedra [MnO_6]. The structure is presented in Fig. 5. It should be noted that the deintercalation of the Li atoms does not fully occurs when charging the battery. The main reasons of this are the structural characteristics and formation of passivating films of by-products which worsen the diffusion on the electrode (solid state)/electrolyte (liquid).

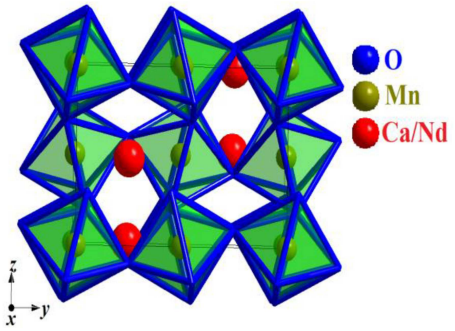

Fig. 5. Crystal structure of the orthorhombic perovskite. Li-insertion occurred into the voids (channels) between the layers of cations (Ca/Nd) and the layers of octahedra [MnO_6].

The decreasing adsorption of the components from electrolyte on the electrode surface and selecting cathode materials with larger channels for intercalation, we can increase the capacity and service life of the battery.

4. Conclusion

The $Li_yCa_xNd_{1-x}MnO_3$ solid solution was synthesized by electrochemical insertion of Li in the structure of $Ca_xNd_{1-x}MnO_3$ oxides (synthesized by solid-state reaction). All phases are characterized by orthorhombic symmetry ($GdFeO_3$-type structure, space group *Pnma*, Pearson's code *oP*20, $Z = 4$). The composition of $Ca_{0.5}Nd_{0.5}MnO_3$, $Ca_{0.3}Nd_{0.7}MnO_3$ and $Ca_{0.05}Nd_{0.95}MnO_3$ samples was confirmed by X-ray fluorescent spectroscopy and energy-dispersive X-ray spectroscopy. Insertion of Li into the voids of oxide phases takes place during the discharge process. The compositions of Li-containing solid solutions are $Li_{0.057}Ca_{0.5}Nd_{0.5}MnO_3$, $Li_{0.091}Ca_{0.3}Nd_{0.7}MnO_3$ and $Li_{0.113}Ca_{0.05}Nd_{0.95}MnO_3$. The scanning electron microscopy method showed the formation of Li-containing aggregates of small block-like particles with dimensions of < 400 nm.

References

[1] S. Yoon, E.H. Otal, A.E. Maegli et al., *Opt. Mater. Express.* **3**, 248 (2013).

[2] P. Kaur, K. Singh, *Ceram. Int.* **46**, 5521 (2020).

[3] M.E. Arroyo-de Dompablo, C. Krich, J. Nava-Avendaño, M.R. Palacín, F. Bardé, *Phys. Chem. Chem. Phys.* **18**, 19966 (2016).

[4] A. Mai, V.A.C. Haanappel, S. Uhlenbruck, Fr. Tietz, D. Stöver, *Solid State Ionics* **176**, 1341 (2005).

[5] J. Han, K. Zheng, K. Świerczek, *Funct. Mater. Lett.* **4**, 151 (2011).

[6] Z. Lu, Fr. Ciucci, *J. Mater. Chem. A* **6**, 5185 (2018).

[7] M. Amores, H. El-Shinawi, I. McClelland et al., *Nat. Commun.* **11,** 6392 (2020).

[8] A. Balińska, V. Kordan, R. Misztal, V. Pavlyuk, *J. Solid State Electrochem.* **19**, 2481 (2015).

[9] G. Kowalczyk, V. Kordan, A. Stetskiv, V. Pavlyuk, *Intermetallics* **70**, 53 (2016).

[10] N.O. Chorna, V.M. Kordan, A.M. Mykhailevych, O.Ya. Zelinska, A.V. Zelinskiy, K. Kluziak, R.Ya. Serkiz, V.V. Pavlyuk, *Vopr. Khim. Khim. Tekhnol.* **2**, 139 (2021).

[11] I. Stetskiv, V. Kordan, I. Tarasiuk, V. Pavlyuk, *Phys. Chem. Solid State* **22**, 577 (2021).

[12] J. Rodriguez-Carvajal, in: *The Satellite Meeting on Powder Diffraction of the XV Congress of the IUCr*, Toulouse 1990, p. 127.

[13] ANR Technologies PTE, Swagelok Type Cells for Lithium Ion Battery Research.

[14] MTech measuring technologies.

[15] V. Kordan, O. Zaremba, P. Demchenko, in: *Int. Conf. on Oxide Materials for Electronic Engineering Fabrication, Properties and Applications*, Lviv 2021, p. 42.